Ecological Modelling 266 (2013) 30–41

Contents lists available at ScienceDirect

Ecological Modelling

journal homepage: www.elsevier.com/locate/ecolmodel

Hydrobal: An eco-hydrological modelling approach for assessing water balances in different vegetation types in semi-arid areas

Juan Bellot[a,c,*], Esteban Chirino[b,c]

[a] Department of Ecology, University of Alicante, Apdo. 99, 03080 Alicante, Spain
[b] Mediterranean Center for Environmental Studies (Foundation CEAM), CEAM, Department of Ecology, University of Alicante, Apdo. 99, 03080 Alicante, Spain
[c] Joint Research Unit University of Alicante, Foundation CEAM, Alicante, Spain

ARTICLE INFO

Article history:
Received 25 August 2012
Received in revised form 18 June 2013
Accepted 1 July 2013
Available online 29 July 2013

Keywords:
Eco-hydrological model
Soil–water content
Vegetation types
Evaporative coefficient
Aquifer recharge

ABSTRACT

In semiarid areas, water is a limited resource and its management is a challenge. Water-balance models can improve the management of water resources by determining the effect of vegetation type on the soil–water balance and aquifer recharge. Here, we present HYDROBAL, an eco-hydrological modelling approach for assessing the water balance with a daily resolution. HYDROBAL is suitable for investigating the temporal variability in soil–water content determined by vegetation water uptake as a function of climatic conditions. The processes, mechanisms, and water flows involved in soil moisture changes are modelled based on daily rainfall and micrometeorological variables and used to predict changes in daily soil–water content. The model outputs include actual evapotranspiration, runoff, and aquifer recharge (deep percolation). The model was applied in a semi-arid area of south-eastern Spain, with six vegetation cover types: bare soil (*B*), open *Stipa tenacissima* steppe (*St*), thorn shrubland (*S*), dry grassland (*G*), and Aleppo pine (*Pinus halepensis*) afforestation of *S* and *G* (*AS* and *AG*, respectively). A dynamic evaporative coefficient (k) was calibrated for each vegetation type to estimate the soil–water consumption. The model was verified in base on its ability to predict the daily measured soil moisture content in plots with different vegetation types. Comparison between the estimated and measured soil moisture contents (θ_{model} vs. θ_{TDR}) indicated good model performance for all vegetation cover types in both wet and dry periods. High value of the coefficient of determination in the linear regressions for $\theta_{model} = f(\theta_{TDR})$ demonstrate the accuracy of the hydrological model. All correlations between measured and predicted soil–water content were strong and significant ($R^2 > 0.69$, $p < 0.001$)

1. Introduction

In recent decades, there has been increasing interest for large-scale water-balance models (e.g., regional, continental) and for long-term studies, both for hydrological purposes and for forest management purposes (Bellot et al., 2001; Evans et al., 1999; Granier et al., 1999). Such extensive applications require robust models that are based on simple soil and vegetation parameters and basic climatic data to let modellers simulate soil–water availability over multi-year periods (Domingo et al., 1999, 2001; Ladekarl, 1998; Steinhardt and Volk, 2003). The literature describes a wide variety of models for hydrological applications (e.g., Arnold et al., 2009; Aydin, 2008; Bornhöft, 1994; Bouten and Jansson, 1995; Delgado et al., 2010; Donker, 2001; Gracia et al., 1999; Jewtti et al., 2004; Kremer and Running, 1996; Morgenstern and Kloss, 1995; Vardavas, 1988), which differ in their objectives, input data, complexity, and spatial and temporal resolution. In some cases, the models have been developed to assess the effects of soil management, to predict the seasonal demand for irrigation, runoff, lake levels, recharge of aquifer systems, and the effects of vegetation on groundwater and sediment production (Arnold et al., 1998, 1999; Aydin, 2008; Brando et al., 2004; Contreras et al., 2008; Onusluel and Rosbjerg, 2010).

In this context, we developed a conceptual modelling approach (HYDROBAL), to quantify the temporal variation of ecosystem water balance as a function of reference evapotranspiration (E_{to}) and soil–water content (*SWC*) in semi-arid areas. HYDROBAL is a model that integrates the meteorological conditions, vegetation characteristics and soil processes to simulate water balances at plot scale in ecosystems dominated by different vegetation types. The model uses a small set of stand parameters (from soil and plant cover) and standard daily meteorological data (reference evapotranspiration and precipitation) as inputs, and estimates the main eco-hydrological terms as outputs: stand evapotranspiration, interception, runoff, deep drainage, and soil–water content.

* Corresponding author. Tel.: +34 96 590 3555; fax: +34 96 590 9832.
E-mail addresses: Juan.Bellot@ua.es (J. Bellot), Esteban.Chirino@ua.es (E. Chirino).

0304-3800/$ – see front matter © 2013 Elsevier B.V. All rights reserved.
http://dx.doi.org/10.1016/j.ecolmodel.2013.07.002

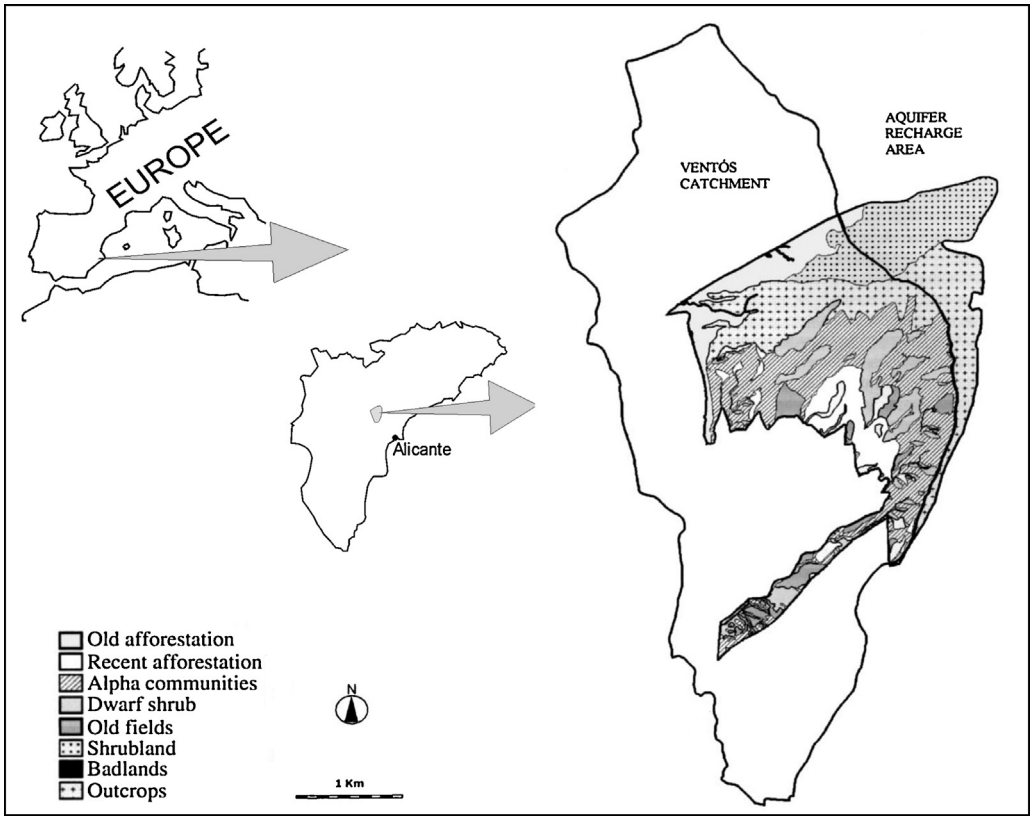

Fig. 1. Localization of Ventós–Castellar aquifer and land cover units on the aquifer recharge area (adapted from Bellot et al., 2001).

Evapotranspiration, which is generally the largest output flux component of the systems, is estimated by the ecophysiological relationships between E_{to} and *SWC*, at a stand scale. These eco-hydrological relationships are determined using an integrative parameter (*k* factor) similar to an evaporative coefficient (Specht, 1972; Specht and Specht, 1993), which is a functional indicator of the canopies transpiration capacity (Boer, 1999; Boer and Puigdefábregas, 2003), based on the average leaf area index (*LAI*) in each vegetation type. The model can be used for different purposes, such as study the impact of land use changes (Bellot et al., 2001) or disturbance due to forest fires on soil–water balance. It also allows computation of integrated water balances across a different vegetation types ranging from bare soil to forest stands.

This paper describes the approach and equations used in the HYDROBAL eco-hydrological model and its application in various vegetation types. Simulations of annual variation in soil–water content are shown for coniferous, shrubland, and grassland vegetation types as well as for bare soil based on the same soil types and climatic conditions. Our final aim is to apply the eco-hydrological model to determine the soil–water balance for six vegetation types in two contrasted climatic years (dry and wet), by assessing the contribution of each vegetation type on actual evapotranspiration, surface runoff, store soil water, and aquifer recharge.

2. Study area

The study area (Fig. 1) is at the Ventós-Agost Aquifer Experimental Station (University of Alicante), which is located in the Municipality of Agost, Alicante Province, in south-eastern Spain (38°28′N; 0°37′W). It covers approximately 1600 ha, with an altitude between 330 and 600 m above sea level, and slopes between 23° and 26°. The climate is semi-arid Mediterranean, with a very high inter-annual variability. The mean annual temperature is 18.2 °C and the annual rainfall is 291.7 mm, most (36%) of which falls in the autumn (Bellot et al., 2001). Marls and limestone are the parent materials, which supports calcareous Cambisols soil (FAO-UNESCO). The soils are shallow (ranging from 0 to 30 cm in depth), with a moderate organic matter content (5.7%), a clay content between 48% and 58%, a soil bulk density of 1.3 g cm^{-3}, and a soil particle density of 2.4 g cm^{-3}. The soil's hydraulic performance is determined by a total porosity of 46.0%, a field capacity of 25.0% (v/v), welting point at 8% (v/v), and an average infiltration rate of 512.6 L m^{-2} h^{-1}. The resistance to penetration measured using a cone penetrometer (at 18% soil moisture content) varies between 31 and 97 kPa (Derouiche, 1996).

3. Vegetation types

On north-facing slopes, the vegetation comprises various land cover types (a patch mosaic) along a successional and structural vegetation complexity landscape: Degraded open land or bare soil (*B*), sometimes covered by microphytic crusts (Bellot et al., 2004); dry grassland (*G*) of *Brachypodium retusum* Pers. Beauv., with dwarf shrubs (*Anthyllis cytisoides* L., *Helianthemum syriacum* (Jacq.) Dum.–Cours., and *Thymus vulgaris* L.); and more mature landscape patches composed of scattered thorn and sclerophyllous shrublands (*S*) with *Quercus coccifera* L., *Pistacia lentiscus* L., *Erica multiflora* L., *Rhamnus lycioides* L., and *Rosmarinus officinalis* L. (Bonet et al., 2001). The dominant anthropic components of the present landscape mosaic are afforested dry grasslands (*AG*) and afforested thorn shrublands (*AS*). On south-facing slopes, the dominant vegetation is a mosaic of open *Stipa tenacissima* steppes (*St*) and dwarf shrubland with gradual transitions between them (Ramírez and Bellot, 2009).

The afforestation was carried out in the early 1960s, as was the case in other regions of Spain (Chirino et al., 2009). The Spanish

Table 1
Summary of some characteristics of plots by vegetation types. Abbreviations: *LAI*: Leaf area index, O.M.: organic matter, d_v: soil bulk density, d_s: soil particle density. (variables for which no units are provided are dimensionless).

		Vegetation types					
		AS	*AG*	*S*	*G*	*St*	*B*
Slope	°	23	21	29	26	25	22
Slope aspect		North	North	North	North	South	North
Vegetation cover	%	95.2	95.8	90.2	70.0	37.0	0.0
LAI	$m^2\ m^{-2}$	3.0	1.7	2.3	1.3	2.1	0.0
pH		8.1	8.1	8.1	8.0	8.1	8.7
O.M.	%	6.91	4.1	6.81	6.5	4.2	4.1
d_v	$g\ cm^{-3}$	1.2	1.2	1.4	1.2	1.2	1.3
d_s	$g\ cm^{-3}$	2.4	2. 5	2.3	2.3	2.3	2.4
Total porosity	%	52.0	51.4	40.6	45.8	49.5	47.1
Fine silt + clay	%	53.1	58. 9	48.6	50.0	58.6	55.4

Forest Service afforested the area with *Pinus halepensis* Miller woodlots over grasslands and degraded shrublands, Afforestation was carried out by manual planting, and actually have a mean density of 1280 ± 692 trees ha^{-1} in grasslands and 2733 ± 1097 trees ha^{-1} in shrublands.

4. Field measurements and laboratory

The research to develop the model was conducted over a 4-year period (from 1996 to 1999). In each vegetation type (*AS*, *AG*, *S*, *G*, *St*, and *B*) we installed three 2×8 m hydrological plots that were randomly distributed within each landscape patch. A summary of some characteristics of the hydrological plots according to vegetation types is shown in Table 1. A soil profile was described morphologically per vegetation type. Soil characteristics for each plot were determined, including texture, bulk density, particle density, total porosity, pH, organic matter, field capacity moisture content and wilting point moisture content (Chirino, 2003). Each hydrological plot was divided into eight subplots ($2\ m^2$) to characterize vegetation in terms of cover (%) of each plant species, stoniness, litter cover and bare soil, as well as, a functional indicator of vegetation community structure like the leaf area index (Chirino et al., 2006).

Precipitation and other daily data of climatic variables (air temperature, relative humidity, solar radiation, and wind) were measured continuously using a CR10 automatic weather station (Campbell Scientific Ltd., Shepshed, Loughborough, UK). After each rain event, rainfall and throughfall were measured; and in each hydrological plot, the runoff and eroded soil were collected and measured in a 2-m-wide Gerlach box installed at the bottom of each plot (Chirino et al., 2006). During two hydrological years (1997/98 and 1998/99), soil–water content was measured weekly, and the day after rainfall events using the Time Domain Reflectometry System (Reflectometer Tektronic 1502C) from 0–30 cm (maximum soil depth). For this purpose, TDR probes were installed at three depths (0–10, 20 and 30 cm), with four replicates per depth in each experimental plot (Chirino, 2003). Sap flow rate was measured in the main species in each season during two years (1998 and 1999) using the stem heat balance method (Chirino et al., 2011). Subsequently, average water consumption for each vegetation type in each plot was determined by means of a scaling up method and weighted based on the % of plant cover and *LAI* of the plot (Chirino, 2003). Infiltration rate in all vegetation types was measured using the two-ring method. With the aim to estimate the throughfall and stemflow and evaluate the importance of different pathways through the canopy, experimental rainfall simulations were made in the laboratory on the main species (*P. halepensis* Miller., *Q. coccifera* L., *P. lentiscus* L., *E. multiflora* L., *S. tenacissima* L., *B. retusum* Pers. Beauv. (Derouiche, 1996).

5. Model operation

The model accounts for the different components of the system, as well as the water flow between them. HYDROBAL simulates the effect of vegetation type and rainfall amount on the soil–water balance and aquifer recharge (Bellot et al., 1998, 2001, 2005; Touhami et al., 2013a). In this section, we describe how the model simulates the processes, mechanisms, and water flows involved in the water balance of several vegetation types. We describe the approach used to simulate the interactions between vegetation structure and the water balance.

HYDROBAL generated, on a daily basis, the water balance for each vegetation type that we analyzed. The outputs are a set of series of values (expressed in $L\ m^{-2}\ day^{-1}$) for the following variables: interception (*Int*), throughfall (*TR*), stemflow (*EF*), net rainfall (*PNt*), surface runoff (R_{off}), stored soil water(*SWs*), reference evapotranspiration (E_{to}), actual evapotranspiration (E_{ta}), direct percolation (*Dp*), slow infiltration (*Si*), deep percolation (*Pc*), and aquifer recharge (*Rec*).

5.1. Model structure and inputs

Programs in C^{++} and Quickbasic software is used to route water flows through the vegetation and soil components of the system (Fig. 2). The main water flows considered are inputs (rainfall) and outputs (evapotranspiration, surface runoff, and deep percolation). The simulated area by the model is a vegetation plot, whose bedrock, soil, and structural plant characteristics must be accounted for.

HYDROBAL's basic structure is based on the previous work of Nizinski and Saugier (1989) and Samper (1997). It has a deterministic and iterative approach in which the variations in soil–water content are calculated at a daily resolution at a plot level using the mass balance Eq. (1), which variables are defined in Table 2.

$$\Delta SWC = P - Int - E_{ta} - R_{off} - Pc \quad (1)$$

The basic data that constitute the model's inputs are presented in Table 2. The weather variables have a daily resolution, the soil characteristics are constant, and the initial stored soil water and water consumption rate (evaporative coefficient, *k*) for each vegetation type are introduced and calibrated parameters, respectively.

5.2. Model calculation: Outputs

The model processes are organized into four independent modules, and the model can be run for any given module without having to run the others. Each module produce output files with daily data that can be used by the module itself or used as inputs for the other modules to initiate the next calculation steps.

Table 2
List of symbols, abbreviations, and units used in the equations of Hydrobal model, climatic variables, soil properties, parameters for calibration and others symbols. (variables for which no units are provided are dimensionless).

Variable type	Measured variables	Abbreviations	Units
Eq. (1) soil–water-balance equation	Soil–water content	ΔWC	$L\,m^{-2}$
	Daily rainfall	P	$L\,m^{-2}$
	Interception	Int	$L\,m^{-2}$
	Actual evapotranspiration	E_{ta}	$L\,m^{-2}$
	Surface runoff	R_{off}	$L\,m^{-2}$
	Deep percolation	Pc	$L\,m^{-2}$
Eq. (2) Penman–Montieth– FAO equation	Potential evapotranspiration	E_{to}	$mm\,day^{-1}$
	Net radiation	R_n	$W\,m^{-2}$
	Heat flow density from the soil	G	$MJ\,m^{-2}\,day^{-1}$
	Temperature	T	°C
	Wind speed	u_2	$m\,s^{-1}$
	Saturation vapor pressure	e_s	kPa
	Actual vapour pressure	e_a	kPa
	Saturation vapor-pressure deficit	$(e_s–e_a)$	kPa
	slope vapour–pressure curve	δ	$kPa\,°C^{-1}$
	Psychometric constant	γ	$kPa\,°C^{-1}$
Eq. (3) Hargreaves–Samani equation	Solar radiation	R_s	$MJ\,m^{-2}\,d^{-1}$
	Temperature-correction factor as a function of H_R	C_t	°C
	Mean temperature	T	°C
	Temperature minimum	T_{min}	°C
	Temperature maximum	T_{max}	°C
Model water flows (Eqs. (4)–(15))	Daily rainfall	P	$L\,m^{-2}$
	Throughfall	TF	$L\,m^{-2}$
	Stemflow	SF	$L\,m^{-2}$
	Interception	Int	$L\,m^{-2}$
	Net rainfall	PNt	$L\,m^{-2}$
	Surface runoff	R_{off}	$L\,m^{-2}$
	Soil–water infiltration	Inf	$L\,m^{-2}$
	Direct percolation	Dp	$L\,m^{-2}$
	Base of natural logarithms	e	2.71828
	Stored soil water	SWs	$L\,m^{-2}$
	Wilting point moisture content (−1500 kPa)	θ_{1500}	%
	Porosity	φ	cm^3
	Usable reserves $(\theta_{33}–\theta_{1500})$	Ru	$L\,m^{-2}$
	Actual evapotranspiration	E_{ta}	$L\,m^{-2}$
	Potential evapotranspiration	E_{to}	$L\,m^{-2}$
	Water consumption rate for each plant cover type	k	
	Field capacity moisture content (−33 kPa)	θ_{33}	%
	Slow infiltration	S_i	$L\,m^{-2}$
	Soil–water availability	SWa	$L\,m^{-2}$
	Deep percolation	Pc	$L\,m^{-2}$
	Aquifer recharge estimate	Rec	$L\,m^{-2}$
	Coefficient of soil–water availability	SWa_coeff	
Daily climatic data	Daily rainfall	P	$L\,m^{-2}$
	Temperature	T	°C
	Relative humidity	H_R	%
	Global radiation	R_g	$W\,m^{-2}$
	Net radiation	R_n	$W\,m^{-2}$
	Wind speed	u_2	$m\,s^{-1}$
	Day number	t	
Soil properties	Wilting point moisture content (−1500 kPa)	θ_{1500}	%
	Field capacity moisture content (−33 kPa)	θ_{33}	%
	Maximum observed soil–moisture content	θ_{max}	%
	Total porosity	P_{total}	%
	Porosity	φ	cm^3
	Organic matter	$O.M.$	%
	Bulk density	d_v	$g\,cm^{-3}$
	Soil particle density	d_s	$g\,cm^{-3}$
	Initial stored soil water	SWs_i	%
Vegetation data	Leaf area index	LAI	$m^2\,m^{-2}$
	Vegetation cover	VC	%
Parameters for calibration	Initial stored soil water	SWs_i	%
	Water consumption rate for each plant cover type	k	
	k factor for dry periods (minimum value)	k_{min}	
	k factor for wet periods (maximum value)	k_{max}	
Other used variables	Difference between initial and final soil moisture	$\Delta\theta$	%
	Stored soil moisture estimated by the model	θ_{model}	%
	Soil–water content observed in the field (from 0 to 30 cm in depth)	θ_{TDR}	%
	Actual evapotranspiration computed from sapflow measurements	$E_{ta\text{-}sf}$	$L\,m^{-2}$
	Actual evapotranspiration estimated by the model	$E_{ta\text{-}model}$	$L\,m^{-2}$

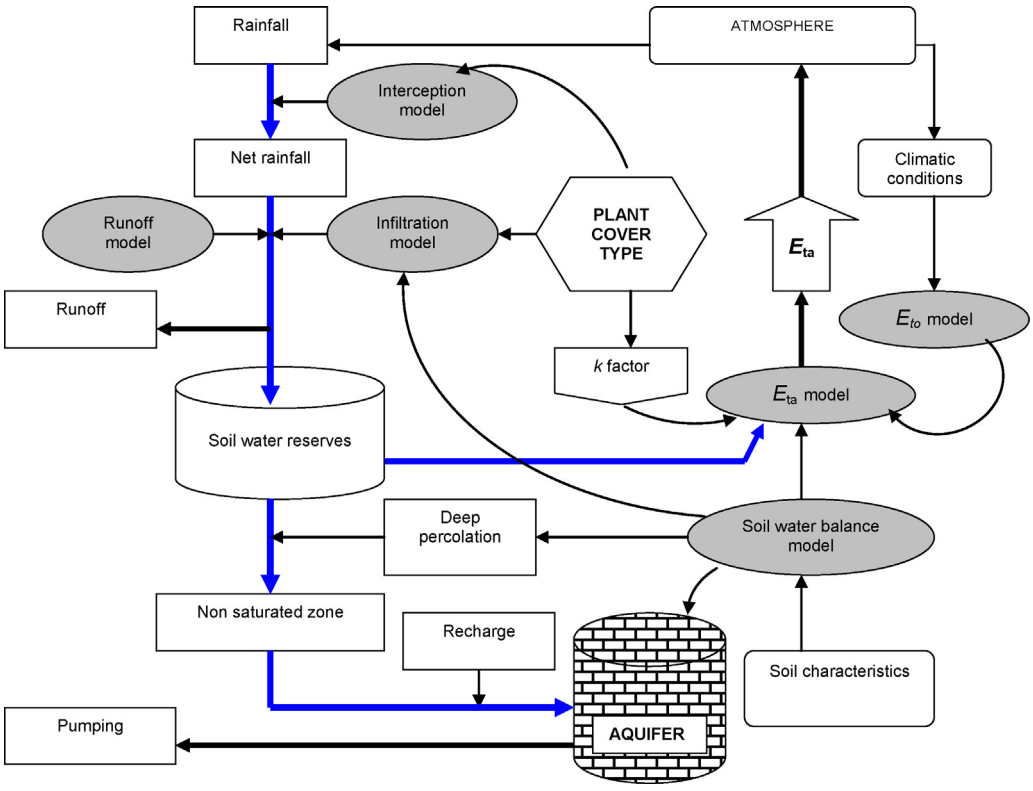

Fig. 2. Flowchart showing the structure of the HYDROBAL model.

5.2.1. Module 1: Reference evapotranspiration

Reference evapotranspiration (E_{to}) was estimated from the climatic data measured above the vegetation canopy and provided by the meteorological station (temperature, relative humidity, total solar radiation, net solar radiation, photosynthetically active radiation, and wind speed). HYDROBAL provides considerable flexibility in the choice of how to calculate E_{to}. Where solar radiation data are available, the Penman–Montieth–FAO method (Eq. (2)) can be used to estimate the reference evapotranspiration (E_{to}). Where only temperature data are available, the Hargreaves–Samani method (Eq. (3)) can be used. In both cases, the input data is a file that contains daily values of these meteorological variables.

Penman–Montieth–FAO equation. This is a modification of Penman's equation, which is used in areas with low moisture stress (Allen et al., 1998)

$$E_{to} = \frac{0.408\,(R_n - G) + \gamma \frac{900}{T+273} u_2\,(e_s - e_a)}{\delta + \gamma(1 + 0.34u_2)} \quad (2)$$

Hargreaves–Samani equation. This equation is empirical in nature and with some modifications (Hargreaves and Samani, 1985) takes the form:

$$E_{to} = 0.0075 \times R_s \times C_t \times T \times (T_{max} - T_{min})^{0.5} \quad (3)$$

When $H_R \geq 54\%$ then $C_t = 0.035 \times (100 - H_R)^{1/3}$
When $H_R < 54\%$ then $C_t = 0.125$

5.2.2. Module 2: Net rainfall

The net rainfall under a canopy is a function of the stand density and age, and is determined by the long-term structural development and seasonal dynamics of the vegetation, which modify the rainfall's physical properties. During the process of interception of the rain by the vegetation, the rain loses part of its kinetic energy before it falls onto a soft, energy-absorbing macro-porous litter layer; if the vegetation and litter are sufficiently abundant, they largely eliminate surface runoff (Wattenbach et al., 2005). The basic vegetation parameter that can be used to describe these effects of the structural characteristics of the canopy is the *LAI* because it is strongly correlated with the amount of rainfall interception, net rainfall and light interception (Bellot and Escarré, 1998; Granier et al., 1999).

The module starts with the gross rainfall (P) received by the vegetation, then distributes it across the vegetation structure as throughfall (TF) and stemflow (SF), which are differentiated according to the canopy stratification of each vegetation type. The estimated values are obtained from the equations of Derouiche (1996), Abdelli (1999), and Chirino (2003), see table in Appendix 1. These values are weighted based on the % cover of the plot by the main species (*P. halepensis, Q. coccifera, P. lentiscus, E. multiflora, B. retusum*, and *S. tenacissima*) for the vegetation types that we analyzed. The input data are daily values of rainfall ($L\,m^2$), and the outputs are daily values of throughfall, stemflow and interception ($L\,m^2$).

Throughfall estimates. Throughfall was estimated using a linear model ($TF = a + b(P)$; P is daily rainfall) obtained from field measurements in the hydrological plots for shrublands, afforested dry grasslands, and afforested thorn shrublands (Chirino, 2003). For the dry grassland and open *S. tenacissima* steppes, the equations were developed based on laboratory simulations using the main herbaceous species in these vegetation types (Abdelli, 1999; Derouiche, 1996). In all cases, the values obtained were weighted according to the % cover by each plant species.

Stemflow estimates: Stemflow was estimated using a linear model ($EF = a + b(P)$; P is daily rainfall). The equations were obtained from laboratory simulations for each species (Abdelli, 1999), and from field work (Bellot and Escarré, 1998; Chirino, 2003); these results were also weighted according to the cover by each species in each plot.

Net rainfall estimates. Net rainfall (*PNt*) was calculated as the sum of *TF* + *EF* (Eq. (4)):

$$PNt_t = TF_t + EF_t \quad (4)$$

Interception estimates. The procedure used for tracking interception (*Int*) of rainfall, followed by storage in and loss from the canopy, is based on the difference between gross precipitation (rainfall, *P*) and net rainfall (*PNt*) during each rainfall event (Eq. (5)). We assumed that this difference represents the integrated value of the maximum canopy storage and the amount of intercepted evaporation from the canopy during storm events.

$$Int_t = P_t - PNt_t \quad (5)$$

5.2.3. Module 3: Surface runoff

Runoff. Surface runoff is calculated by a linear regression as a function of precipitation ($R_{off} = a + b(P)$; *P* is daily rainfall), which is only suitable when daily sums of rainfall are available. It estimates surface runoff as a function of gross rainfall (*P*) in each vegetation type using the equations obtained previously in the hydrological plots by Chirino (2003). The input data are daily values of rainfall ($L\,m^{-2}$), and the outputs are daily values of runoff in each plot of each vegetation type ($L\,m^{-2}$).

5.2.4. Module 4: Water balances in the vegetation plot

Water balances in the vegetation plot is calculated daily according to structure and species composition of the plot. Using the data files generated in the previous three modules (reference evapotranspiration, net rainfall, and surface runoff), HYDROBAL calculates the daily soil–water content.

5.2.5. Soil–water content estimates

To calculate the daily soil–water balance, HYDROBAL utilizes the difference between two values of soil–water contents to represent the plant-extractable water: the lower limit (corresponding to the observed water content at the wilting point in the study area, θ_{1500}, expressed as $L\,m^{-2}$) and the upper drainage limit (corresponding to the field capacity, θ_{33}, expressed as $L\,m^{-2}$). The soil–water content difference between these levels (θ_{33}–θ_{1500}) corresponds to the soil's water storage capacity. The soil–water content in the vertical soil layers is calculated by distributing the total infiltrated water among three 10-cm-think layers by means of a simple cascade; that is, when an upper level reaches field capacity, all additional water "cascades" into the next lowest level. In the water-balance calculation, the soil texture is regarded as being homogeneous throughout the soil profile. The stored soil water is increased by infiltration, which equals net rainfall minus runoff. If the stored soil water in the rooting zone is above field capacity, the surplus water percolates into the subsoil. Water that percolates below the maximum rooting depth of the vegetation cannot be extracted again in later stages of the simulation, and is considered to become the daily aquifer recharge.

5.2.6. Soil–water infiltration

Soil–water infiltration (*Inf*) is calculated to a depth of 30 cm using the daily values of net rainfall and the runoff at a plot level using (Eq. (6), and is commonly referred as the "upper soil storage" (to a depth of 30 cm at our study sites).

$$Inf_t = PNt_t - R_{off_t} \quad (6)$$

Water within this layer percolates downward or is lost to nearby bodies of water by means of deep percolation and lateral interflow, respectively. In the model, downward percolation occurs whenever water infiltration plus the previous soil–water content exceed the soil's field capacity (θ_{33}).

5.2.7. Direct percolation

Based on field observations, many hydrologists suggest that some infiltration water percolates downwards before the soil's field capacity is reached (Samper, 1997). Work done at plot scale showed a strong dependency of direct percolation on the amount of precipitation when the soil–water status changes from dry to wet. The direct percolation (*Dp*) at a depth >30 cm was calculated using (Eq. (7)) as a fraction of the infiltration (*Inf*), which is determined by the stored soil water (*SWs*) and other soil parameters (Eq. (8)). Finally, *Dp* on day *t* decreases the daily *SWs* (Eq. (9)) that is used in calculations for the next day (*t* + 1).

$$Dp_t = Inf_t \times \left(1 - e^{\left(-3\times\left(\frac{\left(SWs - \left(\frac{Ru}{5}\right) + \theta_{1500}\right)}{\left(\phi - \left(\frac{Ru}{5}\right) + \theta_{1500}\right)}\right)\right)}\right) \quad (7)$$

$$SWs_t = SWs_{t-1} + Inf_t \quad (8)$$

$$SWs_{t+1} = SWs_t - Dp_t \quad (9)$$

5.2.8. Actual evapotranspiration estimates: The evaporative coefficient (k factor)

One important assumption of HYDROBAL consists of determining of the evaporative coefficients or *k* factor, which are used to adjust and calibrate the model to account for differences among the vegetation types. This approach accounts for the average water consumption characteristics for each vegetation type, and follows the approach used by Specht (1972), Specht and Specht (1993), and Boer and Puigdefábregas (2003). Daily E_{ta} is calculated as a function of E_{to}, the *k* factor, and stored soil water (SWs_t).

The evaporative coefficient (*k* factor) in this model expresses the transpiration rate capacity characteristic of each vegetation type's, as a function of the plant cover and structure, and soil–water availability (*SWa*). In contrast with the Specht approach, in HYDROBAL it is a dynamic factor that changes daily, ranging between a minimum value (k_{min}) for the driest days and a maximum (k_{max}) for the wettest days. To calculate *k*, it is necessary to first determine the coefficient of soil water availability (*SWa_coeff*), which reflects the daily soil–water availability, using Eq. (10). *k* is daily calculated as a fraction of k_{max}, as described in Eq. (11).

$$SWa\_coeff_t = 1 - \frac{\theta_{33} - SWs_t}{\theta_{33} - \theta_{1500}} \quad (10)$$

$$k = k_{max} \times SWa\_coeff_t \quad (11)$$

Actual evapotranspiration (E_{ta}) is the main water loss in the semi-arid soil–plant system and strongly determines the soil–water content, which is a critical variable for water availability to vegetation and the resulting degree of water stress. We defined the plant community water consumption ($E_{ta;}$ Eq. (12)) as the actual evaporation rate, determined from a combined modification of the Nizinski and Saugier (1989) and Specht (1972) equations, in which E_{ta} is a fraction of E_{to} (the maximum atmospheric demand for water), and the forcing variables are the current value of the stored soil water (*SWs*) and *LAI*, represented by the *k* factor evaporative coefficient.

$$E_{ta\_t} = E_{to\_t} \times \left(1 - e^{(-k\times SWs_t)}\right) \quad (12)$$

5.2.9. Estimates of the stored soil water

The stored soil water (*SWs*. Eq. (13)) is the main water-balance variable used to calibrate and validate the model. The amount of water stored in the soil profile (to a depth of 30 cm in the present study) at the end of day *t* + 1 is calculated from the soil–water reserve of the previous day (*t*), plus the infiltration of day *t*, less the

Table 3
Summary of parameters and *k* factors used for each vegetation type to fit and calibrate the model. θ_{1500}, wilting point moisture content; θ_{33}, field capacity moisture content; θ_{max}, maximum observed soil moisture content; P_{total}, total porosity; SWs_i, initial stored soil water; k_{max}, calibration coefficient for dry minimum; k_{min}, calibration coefficient for dry maximum. Vegetation types: *B*, bare soil; *St*, open *Stipa tenacissima* steppe; *S*, thorn shrubland; *G*, dry grassland; *AS* and *AG*, Aleppo pine (*Pinus halepensis*) afforestation of *S* and *G*, respectively.

Parameters	Vegetation type					
	AS	*AG*	*S*	*G*	*St*	*B*
θ_{1500} (%)	11	12	9	10	7	12
θ_{33} (%)	25	20	24	23	20	20
θ_{max} (%)	35	36	31	33	20	28
P_{total} (%)	52	51	41	46	58	50
SWs_i (%)	11	12	9	10	7	12
k_{min}	0.012	0.009	0.015	0.014	0.010	0.015
k_{max}	0.025	0.020	0.030	0.028	0.015	0.015

outputs by E_{ta} on day *t*. When $SWs_{t+1} > \theta_{33}$, then another soil–water output, slow infiltration (*Si*), is produced.

$$SWs_{t+1} = SWs_t - Et_{a\_t} \quad (13)$$

If $SWs_{t+1} > \theta_{33}$, then $Si_t = SWs_{t+1} - \theta_{33}$ and $SWs_t = \theta_{33}$.

5.2.10. Total deep percolation and aquifer recharge estimates

Both, total deep percolation (*Pc*) and aquifer recharge estimates (*Rec*) are the most difficult variables to estimate from the water balance model, due the absence of field measurements. It is calculated as the sum of two previous variables namely, direct percolation (*Dp*) and slow infiltration (*Si*) when stored soil water exceeded the field capacity. Eq. (14) estimates the total deep percolation for an individual rainfall event, and Eq. (15) estimates the cumulative aquifer recharge that results from deep percolation throughout the simulation period. In both cases, these water amounts represent the aquifer recharge that results from the vertical movement of precipitation, which arrives in the saturated zone after a delay time that is characteristic of the Ventós aquifer in the study area (Andreu et al., 2006; Touhami et al., 2013a).

$$Pc_t = Dp_t + Si_t \quad (14)$$

$$Rec = \sum_{t=1}^{t=n} Pc \quad (15)$$

5.3. Calibration of k factor

To fit the model calculations to the observed data and perform calibration, HYDROBAL uses several parameters (θ_{1500}, θ_{33}, θ_{max}, P_{total}, Rs_i,) from soil characteristics, and calibrate the *k* factor (k_{min}, and k_{max}). In our study, the model was calibrated using the input parameters and *k* factors summarized in Table 3.

In each vegetation type, factor k_{min} was determined from *k* value which produces the best fit in the curve that validates the stored soil water results estimated by the model by comparing them with the soil–water content observed for each vegetation type during a dry period. In our case, derived k_{min} values ranged between 0.009 and 0.015 for the six vegetation types (Table 4).

Factor k_{max} stems from the value of *k* which produces the best fit in the curve that validates the stored soil water results estimated by the model by comparing them with the soil–water content observed for each vegetation type during wet periods. The k_{max} factors we obtained (Table 4) ranged between 0.015 and 0.030. The minimum value was for the *St* and *B* vegetation types.

Soil–water reserves (*Rs*) fluctuate throughout the year. If the difference between θ_{33} and Rs_t is low (Eq. (10)), then the soil water availability (*SWa_coeff*) will be larger and consequently the vegetation's transpiration capacity will be increased (Eq. (11)), and HYDROBAL will assign a high *k* value. Under these conditions, when soil–water reserves are low, we observe the minimum water availability for the plants; the model then uses a value of *k* close to its minimum (k_{min}). Conversely, when soil reserves are high, water availability is higher and the model uses a *k* value close to its maximum (k_{max}).

As we noted previously, the evaporative coefficient *k* represents the vegetation's transpiration capacity as a function of soil–water availability (*SWa_coeff*) and is associated with canopy structures in each of the six vegetation types that we studied. The vegetation structures that maintain a lower soil moisture reserve throughout the time should have a higher k_{max} value. The values of k_{max} used in the model for each vegetation type were contrasted with the average soil moisture content recorded in the field for each vegetation type during two hydrological years (September 1997 to August 1999). The vegetation types with low soil moisture (*S* and *G*) have the highest k_{max} values. Although *St* had the lowest soil moisture, it also had a lower k_{max} value than expected; this can be explained by the fact that soils in the area where *St* vegetation grew (south-facing slopes with higher exposure to the sun) show less soil development and a lower infiltration rate.

To support the relationship between soil moisture and k_{max}, we compared the average soil moisture values with the average water consumption for each vegetation type (Table 4). Vegetation types with lower soil moisture (*St* and *S*) showed higher rates of water consumption, whereas *B* and *AG*, with the highest levels of soil moisture, had the lowest water use (excluding *B*, which had no vegetation). In *G* and *AS*, k_{max} was related more to soil moisture than to estimated water consumption, which is unexpected. In *G*, the high value of k_{max} complements the effect of direct evaporation on soil moisture, which was not accounted for in the water consumption estimates based on from sap flow in this vegetation type (Chirino et al., 2011). In *AS*, the high rate of estimated water consumption was influenced by high water consumption by the areas of shrubland and Aleppo pine, which are thought to absorb the highest amount of water at depths greater than 30 cm, thus the

Table 4
Values of the k_{max} and k_{min} factors (calibration coefficients for dry minimum and wet maximum, respectively), average soil moisture, and average water consumption for each vegetation type. Vegetation types: *B*, bare soil; *St*, open *Stipa tenacissima* steppe; *S*, thorn shrubland; *G*, dry grassland; *AS* and *AG*, Aleppo pine (*Pinus halepensis*) afforestation of *St* and *G*, respectively.

Vegetation type	Average soil moisture	k_{max}	k_{min}	Average water consumption
	(%)			($L\,m^{-2}\,day^{-1}$)
St	12.68	0.015	0.010	0.781
S	15.28	0.030	0.015	0.688
G	16.04	0.028	0.014	0.304
AS	17.36	0.025	0.012	0.806
AG	18.11	0.020	0.009	0.443
B	19.06	0.015	0.015	0.000

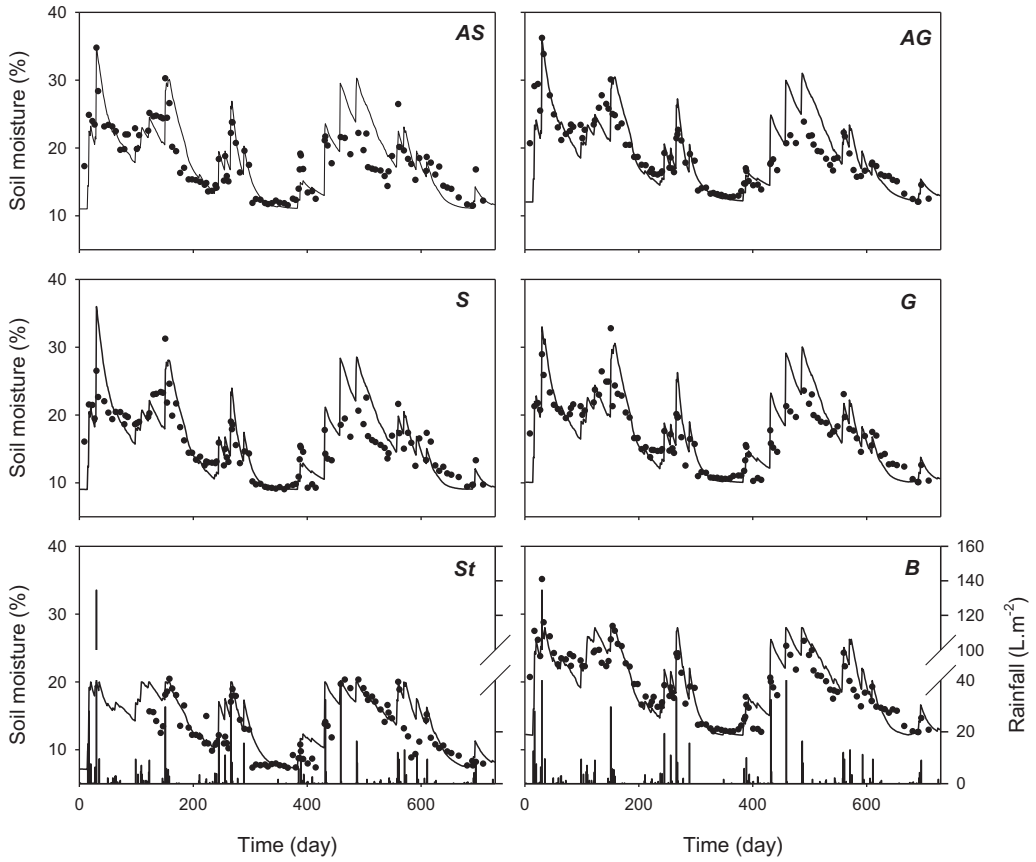

Fig. 3. Results of the fitting and calibration of the eco-hydrological model (HYDROBAL). The daily rainfall is shown by bars; values in the graph represent the measured soil moisture (θ_{TDR}, black circles) and the predicted soil moisture (θ_{model}, solid lines). Days 1 to 365 represent the wet year; days 366 to 730 represent the dry year. Vegetation types: *B*, bare soil; *St*, open *Stipa tenacissima* steppe; *S*, thorn shrubland; *G*, dry grassland; *AS* and *AG*, Aleppo pine (*Pinus halepensis*) afforestation of *S* and *G*, respectively.

effect of this water use could not be detected based on our sampling depth (0 to 30 cm).

5.4. Model verification

To verify the results, by default HYDROBAL performs a graphical and statistical comparison between the daily values of the soil moisture reserves estimated by the model (θ_{model}) and average soil moisture values measured during the monitoring period (mean θ_{TDR} from 0 to 30 cm) for each vegetation type. The graphical representation of these series of values makes it possible to identify the best fit between estimated and observed values for each vegetation type. Also is possible to use other outputs variables estimated by the model (E_{ta}, deep percolation or aquifer recharge, and runoff) to perform graphical and statistical comparison between the daily observed and estimated values.

To assess the reliability of the simulated outputs, we used four statistical methods to compare the simulated and observed results: (1) basic descriptive statistics (i.e., mean, median, maximum, and minimum values and the coefficient of variation), (2) the coefficient of determination (R^2) for simple linear regressions between the observed (θ_{TDR}) and estimated (θ_{model}) soil moisture values (Aydin, 2008), (3) the coefficient of determination for simple linear regressions between the value of actual evapotranspiration estimated by the model ($E_{ta\text{-}model}$) and the transpiration values measured in the vegetation types ($E_{ta\text{-}sf}$) obtained from sapflow measurements during the sampling period (Chirino, 2003; Chirino et al., 2011), and (4) calculation of the root-mean-square error (RMSE) commonly used to test the goodness of fit of simulation models (Basci et al., 1995; Diekkrüger et al., 1995; Eitzinger et al., 2004; Wegehenkel, 2000).

6. Application of HYDROBAL

We applied the model to a set of data from September 1997 to August 1999, which include two very different hydrological years: a wet year (September 1997 to August 1998; rainfall = 426.3 L m^{-2}) and a dry year (September 1998 to August 1999; rainfall = 230.6 L m^{-2}). The application model was done on the data of six vegetation types using the parameter values summarized in Table 4. The comparison of observed soil–water content in the field and daily water content stored, estimated by model for each vegetation type showed consistently good results (Fig. 3).

We verify the results with a simple linear regression of the θ_{model} value (y) as a function of the θ_{TDR} value (x) (Fig. 4) showed highly significant coefficients of determination for all vegetation types ($p < 0.001$). For the *AS, S, G* vegetation types, and bare soil (*B*), the coefficients of determination were higher than 0.70. The mean RMSE for all vegetation types combined was 0.026%. These results support the suitability of the eco-hydrological model for estimating soil moisture reserves and the reliability of its estimates of the remaining output variables. However, our validation of the results based on a comparison between $E_{ta\text{-}model}$ and $E_{ta\text{-}sf}$ did not show a good fit (mean RMSE = 0.105 L m^{-2}). This is probably because $E_{ta\text{-}model}$ was estimated as a continuous function of the soil–water reserve (Eq. (12)), following a pattern similar to that of θ_{model}, whereas the $E_{ta\text{-}sf}$ was measured punctually in some days and extrapolated to all annual period.

6.1. Water balance in different vegetation types

For both years (wet and dry), Table 5 shows that the highest interception values were for vegetation types with taller structures

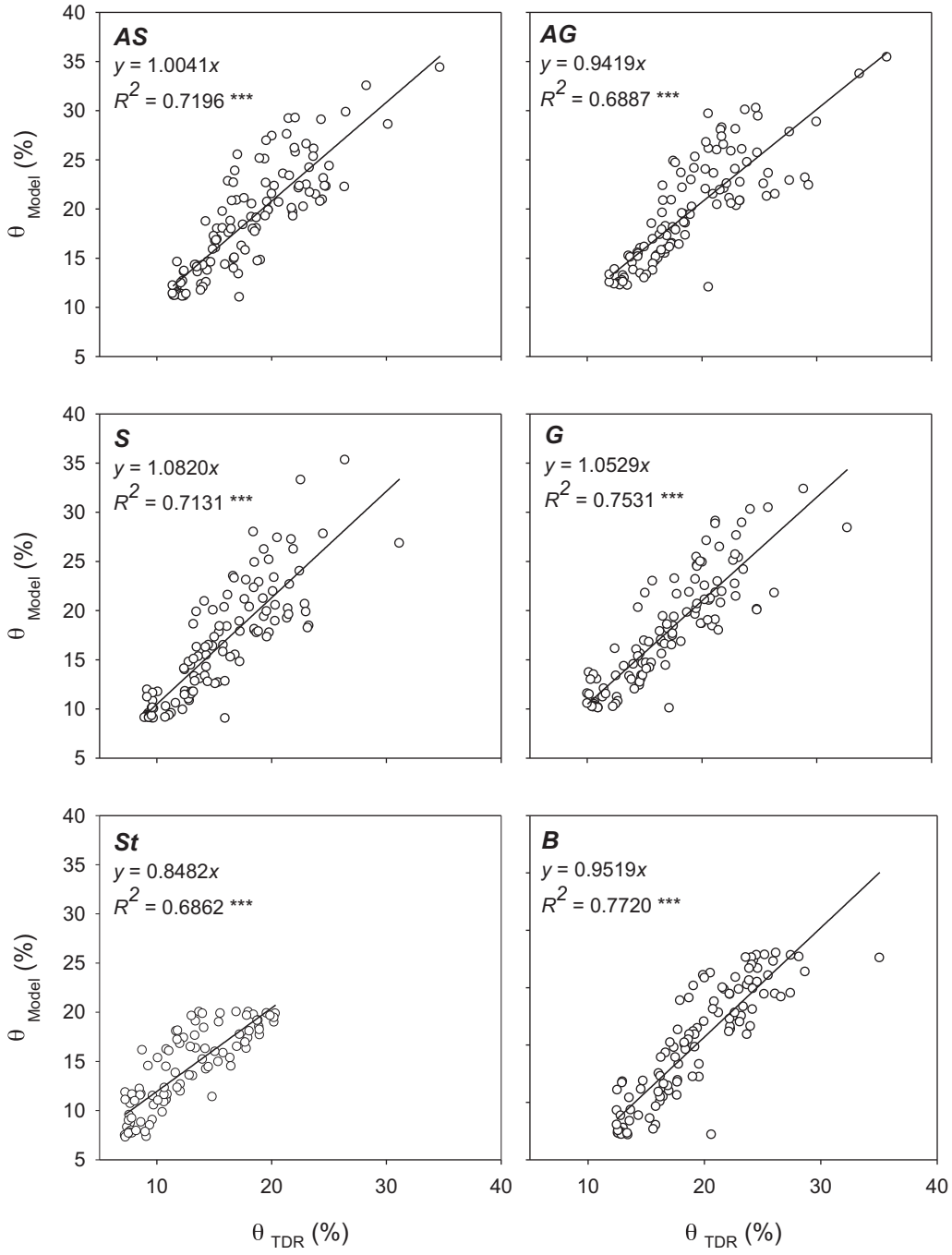

Fig. 4. Validation of the results of the eco-hydrological model (HYDROBAL). We used linear regression to compare the measured soil moisture (θ_{TDR}) with the predicted soil moisture (θ_{model}). We showed the slope (m) of linear equations ($y = mx$) and the coefficient of determination (R^2). Vegetation types: *B*, bare soil; *St*, open *Stipa tenacissima* steppe; *S*, thorn shrubland; *G*, dry grassland; *AS* and *AG*, Aleppo pine (*Pinus halepensis*) afforestation of *S* and *G*, respectively. (*** $p < 0.001$).

and a higher plant cover, with maximum values for the vegetated sites greater than 18% for *AS*, *AG*, and *S* and less than 12% for the other vegetation types in the wet year, versus values greater than 22% for *AS*, *AG*, and *S* and less than 15% for the other vegetation types in the dry year; for *B*, interception was 0% in both years. The high net rainfall values for the vegetated sites (81% to 92% in the wet year and 76% to 90% in the dry year, versus 100% for *B* in both years) showed that the throughfall was the dominant water flow. Soil moisture variations between the initial and final values during the study period ($\Delta\theta$) showed relatively minor accumulation of soil water for the vegetated sites (0.06% to 0.37% in the wet year and 0.29% to 0.67% in the dry year), versus 0.12% and 0.59%, respectively, for *B*. This result agreed with the hydrological year defined in our study, which started after a dry period and ended in the following dry period. The actual evapotranspiration for the vegetated sites (43% to 64% in the wet year and 62% to 78% in the dry year, versus 57% and 79%, respectively, for *B*) was the dominant output flow, followed by aquifer recharge (22% to 43% in the wet year and 4% to 24% in the dry year) and surface runoff (0.41% to 5.29% in the wet year and 0.37% to 2.84% in the dry year), versus 8.3% and 4.7%, respectively, for *B*.

In the dry year, interception and actual evapotranspiration were higher than in the wet year for all vegetation types, and consequently, net rainfall, runoff, and aquifer recharge were lower (Table 5). In contrast, aquifer recharge was higher in the wet year due to the higher net rainfall and lower interception and

Table 5
Results of water balance calculations using the HYDROBAL hydrological model. Output variables are expressed as the proportion (%) of annual rainfall. (The wet year was from September 1997 to August 1998; annual rainfall = 426.3 L m^{-2}, and potential evapotranspiration (E_{to}) = 989.76 L m^{-2}. The dry year was from September 1998 to August 1999; annual rainfall = 230.6 L m^{-2}, and E_{to} = 1021.27 L m^{-2}.) Vegetation types: *B*, bare soil; *St*, open *Stipa tenacissima* steppe; *S*, thorn shrubland; *G*, dry grassland; *AS* and *AG*, Aleppo pine (*Pinus halepensis*) afforestation of *S* and *G*, respectively. *Int*, interception; *PNt*, net rainfall; R_{off}, surface runoff; E_{ta}, actual evapotranspiration; $\Delta\theta$, difference between initial and final soil moisture; *Rec*, aquifer recharge estimate.

Wet year						
Output	Vegetation type					
variable	*AS*	*AG*	*S*	*G*	*St*	*B*
Int	18.28	19.34	18.26	11.46	8.20	0.00
PNt	81.72	80.66	81.74	88.54	91.80	100.00
R_{off}	0.41	0.84	0.61	0.56	5.29	8.33
E_{ta}	58.26	56.66	58.82	64.21	43.43	56.74
$\Delta\theta$	0.18	0.32	0.06	0.09	0.37	0.12
Rec	22.91	22.92	22.24	23.66	42.74	34.70
Dry year						
Output	Vegetation type					
variable	*AS*	*AG*	*S*	*G*	*St*	*B*
Int	22.91	23.85	22.95	14.72	10.43	0.00
PNt	77.09	76.15	77.05	85.28	89.57	100.00
R_{off}	0.37	0.79	0.54	0.56	2.84	4.74
E_{ta}	70.09	67.59	71.64	78.41	62.25	78.91
$\Delta\theta$	0.42	0.61	0.29	0.42	0.67	0.59
Rec	6.10	7.00	4.49	5.77	23.64	15.60

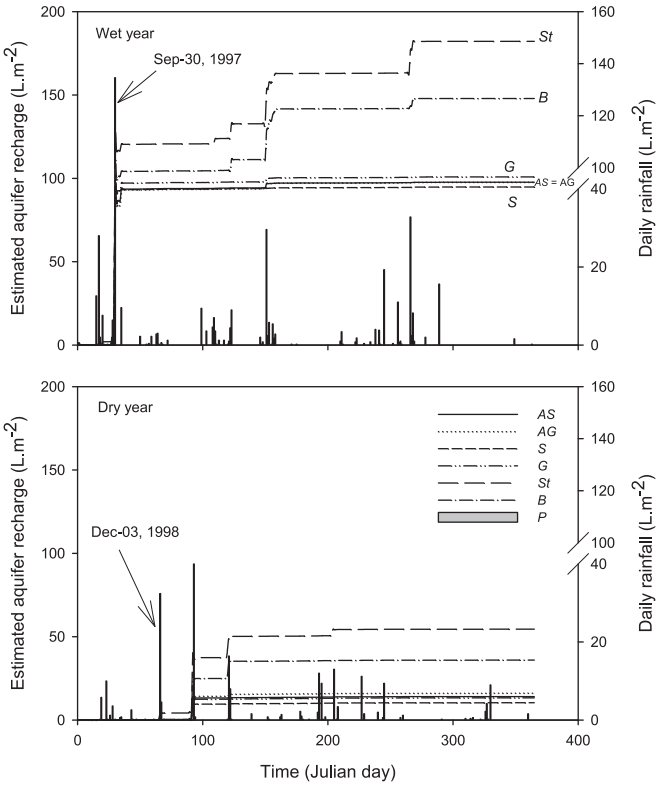

Fig. 5. Daily rainfall and the cumulative daily aquifer recharge for the vegetation types in the wet and dry years. Vegetation types: *B*, bare soil; *St*, open *Stipa tenacissima* steppe; *S*, thorn shrubland; *G*, dry grassland; *AS* and *AG*, Aleppo pine (*Pinus halepensis*) afforestation of *S* and *G*, respectively. (*B*: long dash line, *St*: dash-dot line, *S*: medium dash line, *G*: dash-dot-dot line, *AS*: solid line, *AS*: dotted line and daily rainfall: grey bar).

evapotranspiration. These results can be verified by examining the contribution of each vegetation type to aquifer recharge (Table 5, Fig. 4). In the wet year, the percentage of aquifer recharge (*Rec* = 22% to 43%) was higher than in the dry year (*Rec* = 4.5% to 23.6%), indicating that wet years clearly favour infiltration and thus, aquifer recharge. On the other hand, rainfall events between 10 and 20 L m^{-2} showed very low percolation values. Only the rainfall events equal to or greater than 30 L m^{-2} produced high infiltration values that led to appreciable aquifer recharge (Fig. 5).

Open *S. tenacissima* steppes and bare soil showed the highest aquifer recharge values (43% and 35% of annual rainfall, respectively, in the wet year, versus 24% and 16% in the dry year). Vegetation types with high plant cover (*AS*, *AG*, *S*, and *G*) showed aquifer recharge of approximately 22.0% of annual rainfall in the wet year, but recharge did not exceed 7% of annual rainfall in the dry year. From these results we conclude that structures with lower stratification and % cover (open *S. tenacissima* steppes and bare soil) provide higher aquifer recharge. This result can be explained if we consider the following issues:

1. The scarcity or absence of plant cover will favor higher net rainfall values in comparison with the better-vegetated structures (*AS, AG, S*, and *G*), for which interception may be as high as 24% of annual rainfall.
2. Most (77%) rainfall events in this region generally had low volume (<5 L m^{-2}), low intensity, and short duration. Under these conditions, the taller vegetation types and those with high % cover had higher interception and decreased net rainfall. Conversely, open *S. tenacissima* steppes and bare soil had values of net rainfall of almost 100% of annual rainfall, thereby increasing the soil moisture reserves and producing higher long-term direct percolation, and slower infiltration and deep percolation.
3. In the presence of big rainfall events, open *S. tenacissima* steppes and bare soil showed the highest water losses due to surface runoff. However, the corresponding percolation values were higher than in the other vegetation types, presumably as a result of the higher net rainfall rates. This was demonstrated by an unusually large rainfall event on 30 September 1997 (day 30, Fig. 5, wet year), during which 134.6 L m^{-2} of rain fell, and on 3 December 1998 (day 95, Fig. 5, dry year), during which 46.4 L m^{-2} of rain fell. Both days show differences in the behaviour of each vegetation type during strong rainfall with respect to percolation and aquifer recharge.

7. Discussion

The literature describes a wide variety of models for hydrological applications as we indicated in the introduction section, but in the application of each model, we can find several differences, due to algorithm, equations system, considered biotic and abiotic factors, complexity level of model, environment or ecosystem in which it is used, etc. As an example, we will analyse some models currently used.

In semi-arid region, we can found several hydrological models with different complexity level. DREAM is a semi-distributed hydrological model which presents several similarities to HYDROBAL model (Gigante et al., 2009; Milella et al., 2012). But both show some differences such as the scale of water balance (plots or basin); the equation to determination of actual evapotranspiration, parameters for the characterization of vegetation, and source of *k* factor, between others. VisualBALAN is a hydrological model especially developed to estimate water resources in different hydrological environments. It can determine hydrological balances in the upper soil, the underlying unsaturated zone and the aquifer (Samper et al., 1999). Some applications have been carried out on semiarid region in Spain (Jiménez-Martínez et al., 2010); however a recently article in our study area have demonstrated

the best goodness of HYDROBAL model (Touhami et al., 2013b). On the other hand, we found model with objectives more specifics. OpenLISEM model estimates the relative contribution of rainfall events of different magnitude to soil erosion (Baartman et al., 2012). Other model is focused to analyse the soil moisture dynamics using a simple non-steady numerical ecohydrological model (Pumo et al., 2008). These last models show structural differences and of objectives with HYDROBAL model.

Others models as HYDRUS or DRAINMOD-FOREST are more complex that HYDROBAL and show several differences with our model. HYDRUS is a model more focussed to analyse water and solute movement in unsaturated, partially saturated, or fully saturated porous media (Šimůnek, 2009). In this model, the water flows through of vegetation canopy is not studied. Vegetation factor is considered from the root water and nutrient uptake (Šimůnek and Hopmans, 2009). DRAINMOD-FOREST is a model of great complexity, used for simulating the hydrology, carbon (C) and nitrogen (N) dynamics, and tree growth for drained forest lands under common silvicultural practices (Tian et al., 2012); but have two main difference with HYDROBAL model: (1) DRAINMOD-FOREST is focuses specifically on forests in areas with a high water table—such as the coastal regions, and (2), this model was developed to the regions of southern and south-eastern United States, and has been used in humid subtropical climate (from 970 to 1450 mm). In contrast, HYDROBAL model is focuses on different cover types in areas with a deep water table and was developed in a semiarid region.

HYDROBAL model, show several differences with others models currently used: (1) Is specifically developed to semiarid areas; (2) At the same time, can be applied on several vegetation cover types with different structure and species composition; (3) Use few variables from soil and vegetation to determine the soil–water balance, showing a low complexity level for the run; and (4) and more important, the vegetation factor is highly considered. The vegetation is considered as a plants community with a water consumption capacity (k factor) in proportion to its structural and functional capacity. In the last decade, HYDROBAL model has been successfully applied to analyze the soil–water balance on different vegetation cover types and assess its effects on runoff, deep drainage, evapotranspiration and soil moisture (Bellot et al., 1998; 2001; Chirino, 2003; Touhami et al., 2013a; 2013b).

8. Conclusions

HYDROBAL estimates the flows and water balance for various vegetation types with a daily resolution at a plot level. The evaluation of the model for each type of cover showed acceptable results for two very different hydrological years at our study site. Several results demonstrate the accuracy of the hydrological model: the strong fit between the daily soil moisture reserves estimated by the model and the observed soil moisture values, the high value of the coefficient of determination in the linear regressions for $\theta_{model} = f(\theta_{TDR})$, and the low RMSE value. In summary, we conclude that HYDROBAL is a useful eco-hydrological model for estimating the effects of vegetation type's on soil–water balance and aquifer recharge in semiarid regions such as the study area.

Acknowledgments

This research was partially funded by the Spanish Government, through theMinistry of Science and Innovation (CGL2008-03649), the Ministry of Economy and Competitiveness (ECOBAL project CGL2011- 30531-C02-01; SURVIVE project CGL 2011-30531-C02-02), the Ministry of Environment (ESTRES project, 063/SGTB/2007/7.1) and CONSOLIDER INGENIO 2010 (GRACCIE Project, CSD2007-00067). The Foundation CEAM is partly supported by Generalitat Valenciana, and FEEDBACKS (Prometeo-Generalitat Valenciana) projects.

Appendix A.

Table 1 Equations used in hydrobal model to determine the water flows through of the canopy. ((1)—source Derouiche (1996); (2)—source Abdelli (1999); (3)—source Chirino (2003). P = Daily rainfall). In shrublands and grasslands and according to species composition, the throughfall and stemflow were determined using the equations from rainfall simulation (rainfall intensity = 15 L m^{-2} h^{-1}) by specie determined by Derouiche (1996) and Abdelli (1999). In afforested shrublands, afforested dry grasslands and sclerophyllous shrublands, the throughfall was determined using the equations from measures in the hydrological plots (Chirino, 2003); and the stemflow by means equations by species from Derouiche (1986) and Abdelli (1999). Subsequently, in all cases, the interceptation (Int) was determined by means of the following equation: $Int = P - TR$.

Specie	Equations by variable	
	Stemflow (SF)	Throughfall (TF)
Pinus halepensis (2)	$SF = 0.073 \cdot P - 0.065$ $R^2 = 0.99$	$TF = 0.916 \cdot P - 0.199$ $R^2 = 0.99$
Quercus coccifera (1)	$SF = 0.215 \cdot P - 0.22$ $R^2 = 0.77$	$TF = 0.697 \cdot P - 0.236$ $R^2 = 0.95$
Pistacia lentiscus (1)	$SF = 0.178 \cdot P - 0.115$ $R^2 = 0.88$	$TF = 0.80 \cdot P - 0.12$ $R^2 = 0.99$
Erica multiflora (1)	$SF = 0.224 \cdot P - 0.247$ $R^2 = 0.97$	$TF = 0.754 \cdot P - 0.025$ $R^2 = 0.99$
Stipa tenacissima (2)	$EC + TR = 0.974 \cdot P - 0.593$ ($R^2 = 0.99$)	
Brachypodium retusum (1)	$EC + TR = 0.794 \cdot P - 0.696$ ($R^2 = 0.98$)	
Afforested shrublands (3)		$TF = 0.605 \cdot P - 1.080$ $R^2 = 0.94$
Afforested dry grasslands (3)		$TF = 0.668 \cdot P - 0.821$ $R^2 = 0.96$
Sclerophyllous shrublands (3)		$TF = 0.645 \cdot P - 0.43$ $R^2 = 0.95$

References

Abdelli F. Análisis comparativo de distintas comunidades vegetales a la distribución del agua de lluvia, a la conservación del agua en el suelo y a la recarga de acuíferos en medios semiáridos. M.Sc. thesis dissertation, Instituto Agronómico Mediterráneo de Zaragoza (IAMZ). 1999; p. 160.

Allen R.G., Pereira L.S, Raes D, Smith M., 1998. Crop Evapotranspiration—Guidelines for Computing Crop Water Requirements—FAO Irrigation and Drainage. Paper no. 56. Rome, Italy,1998.

Andreu JM, Linares J, Pulido-Bosch A, García-Sánchez E, Bellot J. Utilización de registros automatizados para el conocimiento de la infiltración en un pequeño acuífero kárstico mediterráneo: ejemplo del Ventós (Alicante, España). En: Durán, J.J., Andreo, B., Carrasco, F. (Eds.). *Karst, cambio climático y aguas subterráneas*. Publ. IGME. Ser: Hidrogeología y Aguas Subterráneas. N(18. Madrid; 2006; 193–202.

Arnold, J.G., Srinivasan, R., Muttiah, R.S., Allen, P.M., 1999. Continental scale simulation of the hydrologic balance. J. Am. Water Resour. Assoc. 35 (5), 1037–1051.

Arnold, J.G., Srinivasan, R., Muttiah, R.S., Willians, J.R., 1998. Large area hydrologic modeling and assessment. Part 1: Model development. J. Am. Water Resour. Assoc. 35 (1), 73–89.

Arnold, S., Attinger, S., Frank, K., Hildebrandt, A., 2009. Parameterization and uncertainty in coupled ecohydrological models. Hydrol. Earth Syst. Sci. Discuss. 6, 4155–4207.

Aydin, M., 2008. A model for evaporation and drainage investigations at ground of ordinary rainfed-areas. Ecol. Modell. 217, 148–156.

Baartman, J., Jetten, V., Ritsema, C., Vente, J., 2012. Exploring effects of rainfall intensity and duration on soil erosion at the catchment scale using openLISEM: Prado catchment, SE Spain. Hydrol. Process. 26, 1034–1049.

Basci, Z., Zemankovic, F., 1995. Validation an objective tool? Results on a winter wheat simulation model application. Ecol. Modell. 81, 251–263.

Bellot, J., Bonet, A., Sánchez, J.R., Chirino, E., 2001. Likely effects of land use changes on the runoff aquifer recharge in a semiarid landscape using a hydrological model. Landscape Urban Plan. 778, 1–13.

Bellot, J., Maestre, F., Chirino, E., Hernández, N., Ortiz de Urbina J.M., 2004. Afforestation with *Pinus halepensis* reduces native shrub performance in a Mediterranean semiarid area. Acta Oecol. 25, 7–15.

Bellot J, Chirino E, Sánchez JR., 2005. The VENTOS Hydrological Model for Water Balance in Different Types of Plant Cover in Semi-Arid Area. Deliverable 8. The AQUADAPT project. EVK1-CT-2001-00104. CD, University of Crandfield, 2005.
Bellot, J., Escarré, A., 1998. Stemflow and throughfall determination in a resprouted Mediterranean holm-oak forest, and changes by precipitation trends. Ann. Sci For. 55 (7), 847–865.
Bellot, J., Sánchez, J.R., Bonet, A., Chirino, E., Abdelli, F., Hernández, N., et al., 1998. Effect of different vegetation type cover on the soil water balance in semiarid areas of south-eastern Spain. Phys. Chem. Earth Part B 24 (4), 353–357.
Boer M., 1999. Assessment of Dryland Degradation. Linking Theory and Practice Through Site Water Balance Modelling. Ph.D. Dissertation. Department of Physical Geography, Utrecht University, The Netherland.
Boer, M.M., Puigdefábregas, J., 2003. Predicting potential vegetation index values as a reference for the assessment and monitoring of dryland condition. Int. J. Remote Sens. 24, 1135–1141.
Bonet, A., Peña, J., Bellot, J., Cremades, M., Sánchez, J.R., 2001. Changing vegetation structure and landscape patterns in semi-arid Spain. In: Villacampa, E.Y., Brebbia, C.A., Usó, J.L. (Eds.), Ecosystems and Sustainable Development III. Advances in Ecological Sciences 10. WITpress, Southampton, pp. 377–385.
Bornhöft, D., 1994. A simulation model for the description of the one-dimensional vertical soil water flow in the unsaturated zone. Ecol. Modell. 7, 5–76, 269-78.
Bouten, W., Jansson, P.E., 1995. Water balance of the Solling spruce stand as simulated with various forest–soil–atmosphere models. Ecol. Modell. 83, 245–253.
Brando, V.E., Ceccarelli, R., Libralato, S., Ravagnan, G., 2004. Assessment of environmental management effects in a shallow basin using mass-balance models. Ecol. Modell. 172, 213–232.
Chirino E, 2003. Influencia de las precipitaciones y de la vegetación en el balance hídrico superficial y la recarga de acuíferos en clima semiárido. PhD Dissertation, Universidad de Alicante, Spain. http://rua.ua.es/dspace/handle/10045/3386
Chirino, E., Bellot, J., Sánchez, J.R., 2011. Daily sap flow rate as an indicator of drought avoidance mechanisms in five Mediterranean perennial species in semi-arid southeastern Spain. Trees-Struct. Funct. 25, 593–606.
Chirino, E., Bonet, A., Bellot, J., Sánchez, J.R., 2006. Effects of 30-years-old Aleppo pine plantations on runoff, soil erosion, and plant diversity in a semi-arid landscape in south-eastern Spain. Catena 65, 19–29.
Chirino, E., Vilagrosa, A., Cortina, J., Valdecantos, A., Fuentes, D., Trubat, R., et al., 2009. Ecological restoration in degraded drylands: the need to improve the seedling quality and site conditions in the field. In: Grossberg, S.P. (Ed.), Forest Management. Nova Science Publishers, New York, pp. 85–158.
Contreras, S., Boer, M.M., Alcalá, F.J., Domingo, F., García, M., Pulido-Bosch, A., Puigdefábregas, J., 2008. An ecohydrological modelling approach for assessing long-term recharge rates in semiarid karstic landscapes. J. Hydrol. 351, 47–57.
Delgado, J., Llorens, P., Guillaume, N., Calder, I.R., Gallart, F., 2010. Modelling the hydrological response of a Mediterranean medium-sized headwater basin subject to land cover change: the Cardener river basin (NE Spain). J. Hydrol. 383, 125–134.
Derouiche A., 1996. Estimation et modelisation des composantes du bilan hidrique chez differentes firmatios arborees, arbustives et herbacees mediterraneennes. M.Sc. Thesis Dissertation, Instituto Agronómico Mediterráneo de Zaragoza (IAMZ), Departamento de Ecología. Universidad de Alicante. 158 pp.
Diekkrüger, B., Soendgerath, D., Kersebaum, K.C., McVoy, C.W., 1995. Validity of agroecosystem models a comparison of results of different models applied to the same data set. Ecol. Modell. 81, 3–29.
Domingo, F., Villagarcía, L., Brenner, A.J., Puidefábregas, J., 1999. Evapotranspiration model for semi-arid shrub-lands tested against data from SE Spain. Agric. For. Meteorol. 95, 67–84.
Domingo, F., Villagarcía, L., Boer, M.M., Alados-Arboledas, L., Puigdefábregas, J., 2001. Evaluating the long-term water balance of arid zone stream bed vegetation using evapotranspiration modelling and hillslope runoff measurements. J. Hydrol. 243, 17–30.
Donker, N.H.W., 2001. A simple rainfall-runoff model based on hydrological units applied to the Teba catchment (South-east Spain). Hydrol. Process. 15, 135–149.
Eitzinger, J., Trnka, M., Hösch, J., Žalud, Z., Dubrovský, M., 2004. Comparison of CERES, WOFOST and SWAP models in simulating soil–water content during growing season under different soil conditions. Ecol. Modell. 171, 223–246.
Evans, S.P., Mayr, T.R., Hollis, H.M., Brown, C.D., 1999. SWBCM: a soil water balance capacity model for environmental applications in the UK. Ecol. Modell. 121 (1), 17–49.
Gigante, V., Iacobellis, V., Manfreda, S., Milella, P., Portoghese, I., 2009. Influences of leaf area index estimations on water balance modeling in a Mediterranean semi-arid basin. Nat. Hazard. Earth Syst. Sci. 9, 979–991.
Gracia, C.A., Tello, E., Sabaté, S., Bellot, J., et al., 1999. GOTILWA. an integrated model of water dynamics and forest growth. In: Rodà, F. (Ed.), Ecology of Mediterranean Evergreen Oak. Forests. Ecological Studies, 137. Springer Verlag, Berlin, Heidelberg, pp. 163–179.
Granier, A., Bréda, N., Biron, P., Villette, S., 1999. A lumped water balance model to evaluate duration and intensity of drought constraints in forest stands. Ecol. Modell. 116 (2-3), 269–283.
Hargreaves, G.H., Samani, Z.A., 1985. Reference crop evapotranspiration from temperature. Trans. ASAE. 1 (2), 96–99.
Jewtti, G.P.W., Garratt, J.A., Calder, I.R., Fuller, L., 2004. Water resources planning and modeling tools for the assessment of land use change in the Luvuvhu catchment, South Africa. Phys. Chem. Earth 29, 1233–1241.
Jiménez-Martínez, J., Candela, L., Molinero, J., Tamoh, K., 2010. Groundwater recharge in irrigated semi-arid areas: quantitative hydrological modelling and sensitivity analysis. Hydrogeol. J. 18, 1811–1824.
Kremer, R.G., Running, S.W., 1996. Simulating seasonal soil water balance in contrasting semiarid vegetation communities. Ecol. Modell. 84, 151–162.
Ladekarl, U.L., 1998. Estimation of the components of soil water balance in a Danish oak stand from measurements of soil moisture using TDR. For. Ecol. Manage. 104, 227–238.
Morgenstern, M., Kloss, R., 1995. Simulation of the soil water balance on the Intensive Loam Site. Ecol. Modell. 81, 41–52.
Milella, P., Bisantino, T., Gentile, F., Iacobellis, V., Trisorio, G., 2012. Diagnostic analysis of distributed input and parameter datasets in Mediterranean basin streamflow modeling. J. Hydrol. 47, 2–473, 262–276.
Nizinski, J., Saugier, B., 1989. A model of transpiration and soil-water balance for a mature oak forest. Agric. For. Meteorol. 47, 1–17.
Onusluel, G., Rosbjerg, D., 2010. Modelling of hydrologic process and potential response to climate change through the use of a multisite SWAT. Water Environ. J. 24, 21–31.
Pumo, D., Viola, F., Noto, L.V., 2008. Ecohydrology in Mediterranean areas: a numerical model to describe growing seasons out of phase with precipitations. Hydrol. Earth Syst. Sci. 12, 303–316.
Ramírez, D.A., Bellot, J., 2009. Linking population composition and habitat structure to assess ecophysiological spatio-temporal responses in Spanish semiarid steppes. Plant Ecolog. 200, 191–204.
Samper, F.J., 1997. Métodos de evaluación de la recarga por la lluvia por balance de agua: utilización, calibración y errores. In: Custodio, E., Llamas, M.R., Samper, J. (Eds.), La evaluación de la recarga a los acuíferos en la planificación hidrológica. Instituto Tecnológico y Geominero de España, Madrid, pp. 41–81.
Samper J, Huguet L, Ares J, García-Vera MA. Manual del usuario del programa VISUAL BALAN v.1.0: Código interactivo para la realización de balances hidrológicos y la estimación de la recarga (VISUAL BALAN v1.0 user manual: an Interactive code for water balance and recharge estimation). Technical Publication ENRESA, Madrid (in Spanish). 1999.
Šimůnek, J., 2009.Development and Application of the Coupled Vadose Zone-Ground Water Flow Modelling Environment: Hydrus Package for MODFLOW Report, University of California Water Resources Center, 112, 55—56, 2009.
Šimůnek, J., Hopmans, J.W., 2009. Modelling compensated root water and nutrient uptake. Ecol. Modell. 220 (4), 505–521.
Specht, R.L., 1972. Water use by perennial evergreen plant communities in Australia and Papua New Guinea. Aust. J. Bot. 20, 273–299.
Specht, A., Specht, R.L., 1993. Species richness and canopy productivity of Australian plant communities. Biodivers. Conserv. 2, 152–167.
Steinhardt, U., Volk, M., 2003. Meso-scale landscape analysis based on landscape balance investigations: problems and hierarchical approaches for their resolution. Ecol. Modell. 168, 251–265.
Tian, S., Youssef, M.A., Skaggs, R.W., Amatya, D.M., Chescheir, G.M., 2012. DRAINMOD-FOREST. Integrated modeling of hydrology, soil carbon and nitrogen dynamics, and plant growth for drained forests. J. Environ. Qual. 41 (3), 764–782, http://dx.doi.org/10.2134/jeq2011.0388.
Touhami, I., Andre, J.M., Chirino, E., Sánchez, J.R., Moutahir, H., Pulido-Bosch, A., Martinez-Santos, P., Bellot, J., 2013a. Recharge estimation of a small kartic aquifer in a semiarid Mediterranean region (southeastern Spain) using a hydrological model. Hydrol. Processes 27, 165.
Touhami, I., Andreu, J.M., Chirino, E., Sánchez, J.R., Pulido-Bosch, A., Martínez-Santos, P., Moutahir, H., Bellot, J., 2013b. Comparative performance of soil water balance models in computing semiarid aquifer recharge. Hydrol. Sci. J., http://dx.doi.org/10.1080/02626667.2013.802094.
Vardavas, I.M., 1988. A simple water balance daily rainfall-runoff model with application to the tropical Magela Creek catchment. Ecol. Modell. 42, 245–264.
Wattenbach, M., Hatterman, F., Weng, R., Wechsung, F., Krysanova, V., Badeck, F., 2005. A simplified approach to implement forest eco-hydrological properties in regional hydrological modelling. Ecol. Modell. 187 (1), 49–50.
Wegehenkel, M., 2000. Test of a modelling system for simulating water balances and plant growth using various different complex approaches. Ecol. Modell. 129 (1), 39–64.